Modelling of soil-structure interaction for seismic analyses of the Izmit Bay Bridge

Modélisation de l'interaction sol-structure pour l'analyse sismique du pont de la baie d'Izmit

Lyngs J. H., Kasper T., Bertelsen K.S.
COWI A/S, Denmark

ABSTRACT: The Izmit Bay Bridge will carry the new Gebze-Orhangazi-Bursa-İzmir motorway across the Sea of Marmara at the Bay of Izmit, Turkey. The suspension bridge with 1550 m long main span will be subjected to strong seismic events. The tower foundations are prefabricated reinforced concrete caisson structures that are installed on prepared gravel beds on Pleistocene deposits, reinforced by driven steel pile inclusions. The design allows for limited permanent displacements in the subsoil and in the gravel-caisson interface during high magnitude seismic events, in order to limit the forces imposed on the superstructure. The displacements and forces in the bridge during seismic events are calculated in displacement-based time history analyses in a global finite element model. This paper describes how the behaviour of the gravel bed and the reinforced subsoil is modelled by distributed sets of vertical and horizontal translational springs, dashpots and gapping elements. The nonlinear horizontal springs are based on hyperbolic relations, generalised in two dimensions, coupled with the local vertical stress and capable of producing hysteresis according to the extended Masing rules. The paper demonstrates an advanced, yet feasible, modelling method that has been put into practice.

RÉSUMÉ : Le pont de la baie d'Izmit portera la nouvelle autoroute Gebze-Orhangazi-Bursa-Izmir dans la baie d'Izmit en Mer Marmara, en Turquie. Le pont suspendu avec une travée principale 1550 m de long sera soumis à de fortes contraintes sismiques. Les fondations des pylônes sont des caissons en béton armé préfabriqués installés sur des assises granulaires préparées sur les dépôts du Pléistocène renforcés par des pieux en acier. Afin de réduire les forces exercées sur la superstructure lors d'événements sismiques de magnitude élevée, le concept de fondation autorise des déformations permanentes à l'interface entre le caisson et l'assise granulaire ainsi que dans les matériaux du sol naturel. Les déformations et efforts dans la superstructure lors d'événements sismiques sont calculés sur la base d'accélérogrammes de déplacements dans un modèle global aux éléments finis. Cet article décrit les méthodes de modélisation du comportement de l'assise granulaire et du sol renforcé par un ensemble de ressorts verticaux et horizontaux, amortisseurs et ouvertures. La modélisation des ressorts horizontaux non-linéaires est basée sur des relations hyperboliques, généralisées en deux dimensions, associées à la contrainte verticale locale et capable de produire une hystérésis selon les règles généralisées de Masing. L'article montre une méthode de modélisation complexe, néanmoins réalisable et qui a été mise en pratique.

KEYWORDS: Foundation design, Suspension bridge, Seismic time history analysis, Soil-structure interaction, Finite element

MOTS-CLÉS : Études des fondations, Pont suspendu, Analyse sismique par accélerogramme, Interaction sol-structure, Éléments finis

1 INTRODUCTION

The Izmit Bay Bridge, shown in Figure 1, is a suspension bridge with a steel superstructure

The bridge is currently under construction and has a 1550 m main span and two 566 m long side spans. The bridge deck is a steel box girder, which carries six road lanes and is located between 60 and 80 m above the sea level. The top elevation of the tower is 252 m above the sea level. Each tower has two steel legs and two steel cross-beams, and their foundations consist of a pre-fabricated concrete caisson placed on a gravel bed on improved soil at 40 m water depth. The anchorages of the bridge are concrete gravity structures.

Figure 1. Global geometry model of the bridge.

The project site in the north-western part of Turkey is located in the area of the North Anatolian Fault with high seismicity. The North Anatolian Fault stretches over approximately 1600 km in east-western direction along the Black Sea coast of Turkey. It is a major right lateral strike slip fault that forms the tectonic boundary between the Eurasian Plate and the Anatolian block of the African Plate. The North Anatolian Fault zone forms a narrow band that splays into three strands in the eastern Marmara Sea region. The northern strand occupies the Izmit Bay and projects across the project alignment, presenting the greatest seismogenic hazard source in the site area. A number of earthquakes with moment magnitudes M_w between 7 and 8 have been recorded in the region. A project-specific seismic hazard study has been carried out based on a detailed review of the literature.

Three different seismic events with different return periods and seismic performance criteria were defined as a basis for the seismic design of the bridge: For the Functional Evaluation Earthquake (FEE) with a return period of 150 years, immediate access to normal traffic and minimal damage (essentially elastic performance) are required. For the Safety Evaluation Earthquake (SEE) with a return period of 1000 years, limited access within days, full service within months and repairable damage without closure to traffic are required. For the No Collapse Earthquake (NCE) with a return period of 2475 years, significant damage without collapse is allowed. For the FEE, SEE and NCE, the rock outcrop peak ground acceleration is 0.25g, 0.65g and 0.87g, respectively.

Time history analyses with a global finite element model (cf. Figure 3) formed the basis for the seismic design of the bridge. For each of the three seismic events, seven sets of near surface displacement time histories with three orthogonal components were derived from site response analyses for each bridge foundation.

This paper focuses on the soil-structure interaction modelling of the tower foundations by means of distributed sets of vertical and horizontal translational springs, dashpots and gapping elements, which form the support of the tower foundation caissons in the global model and to which the

displacement time histories are applied in the seismic analyses. The springs, dashpots and gapping elements have been derived to provide a realistic, best-estimate representation of the nonlinear soil-structure interaction during seismic events based on unfactored material parameters.

2 TOWER FOUNDATIONS

The concept of limiting the seismic forces in the superstructure by seismic base isolation of the bridge piers (FIB 2007) has previously been used e.g. for the Rion-Antirion cable-stayed bridge in Greece (Yang et al. 2001). The pier foundations were placed on a gravel bed on soil improved with steel pile inclusions, which are not connected to the foundations. Such a solution allows for rocking, gapping and sliding of the foundations. The same concept is used for the tower foundations of the Izmit Bay Bridge.

The tower foundation caissons with a 54 x 67 m footprint area are placed on a 3 m thick gravel bed, as shown in Figure 2. 13 x 15 rows of 2.0 m diameter and 34.25 m long driven steel pile inclusions with wall thicknesses of 20 to 25 mm are used to improve the subsoil under each caisson in order to provide sufficient bearing capacity and limit the permanent displacements within the subsoil under ship impact and seismic events.

The ground conditions of the tower foundations are characterised by sand and clay layers. The spacing of the pile inclusions is 5 m in both directions. The pile inclusions stop within the gravel bed, 0.75 m below the gravel bed surface.

3 MODELLING CONCEPT

In order to model the above mentioned foundation characteristics in sufficient detail, a finite element representation of the soil-foundation interface is developed and implemented in COWI's FE-software for bridges, IBDAS (Sørensen et al. 1990). Special features for this soil-foundation model include:

- Use of distributed foundation supports
- Horizontal response coupled to vertical force
- Non-linear, hysteretic spring formulation
- Two-dimensional generalisation of springs

3.1 *Global model*

The global finite element model is established in IBDAS (cf. Figure 3). The entire bridge is described in a single model, capable of non-linear construction phase modelling, response spectrum analysis as well as fully non-linear time domain calculations.

3.2 *Distributed supports*

In typical applications for global modelling, the soil-structure interface of a caisson may be represented by a single-point support stiffness matrix, see e.g. (Lam et al. 2007).

The principle is shown to the left in Figure 4. By modelling the interface as single-point support, the foundation bottom must be modelled as a rigid structure, which implies that no stresses inside the concrete caisson are calculated directly.

In order to generate such stresses directly during time domain analyses, and to provide a detailed modelling of the nonlinear behaviour under combined loading, it has been decided to use distributed springs, as sketched to the right in Figure 4.

In Figure 4, the springs are shown as single sets of springs, for simplicity. Actually, for each spring-supported part of the foundation area, a full set of horizontal and vertical springs and dashpots is assigned, as sketched in Figure 5.

As a sufficiently accurate approximation, all sets of distributed springs are defined identical, with no variation with respect to the location below the foundation base plate. The discretization of the distributed supports was investigated, and it has been found that a 13-by-15 grid provided sufficient resolution and accuracy.

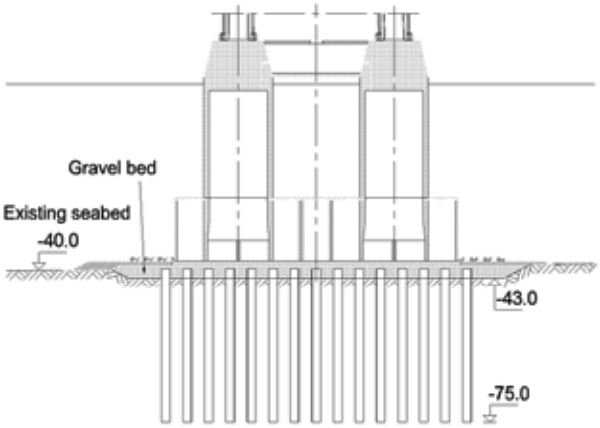

Figure 2. Tower foundation vertical section.

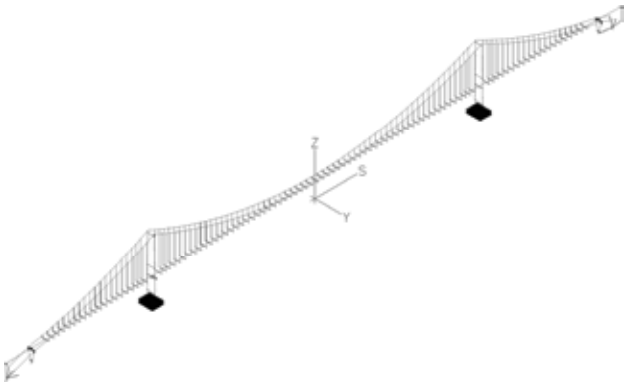

Figure 3. IBDAS global finite element model of the bridge.

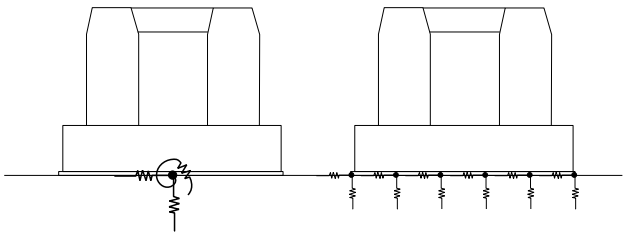

Figure 4. Principle of "single-point support" (left) and "distributed supports" (right).

3.2.1 *Vertical elements*

The vertical elements consist of two linear springs coupled in series, a dashpot and a gapping element, cf. Figure 5. The purpose of having two springs is to make it possible to distinguish between the response in the gravel bed and in the reinforced soil below the gravel bed. Since both springs are linear, both material and radiation damping are included in the dashpot. It has been evaluated that the linear approach provides a very reasonable approximation to the push-over response, cf. Section 4.2.

3.2.2 *Horizontal elements*

The horizontal elements consist of two non-linear springs, cf. Figure 5. The backbone curve for the gravel spring is defined as a function of the vertical force measured at the gapping element, by the expression:

$$F_y = \frac{k_{h0,\text{gravel}} \cdot A_{\text{rep}} \cdot y}{1 + \left(\frac{k_{h0,\text{gravel}} \cdot A_{\text{rep}}}{\mu \cdot F_z} \cdot |y|\right)}$$

where y is the horizontal translational coordinate, F_y is the horizontal force, F_z is the force in the associated vertical spring, $\mu = 0.7$ is the interface friction coefficient, k_{h0} is the initial stiffness and A_{rep} is the representative foundation area covered by the spring set.

The soil spring is defined from the same principle, but independent of the vertical force:

$$F_y = \frac{k_{h0,\text{soil}} \cdot A_{\text{rep}} \cdot y}{1 + \left(\frac{k_{h0,\text{soil}}}{\tau_{\max}} \cdot |y|\right)}$$

where $\tau_{\max}$ is a maximum shear stress.

Unloading and reloading is defined with hysteretic behaviour. Since material damping is embedded in the hysteretic behaviour, the dashpot only includes radiation damping.

3.3 *Hysteretic behaviour*

All nonlinear springs are defined with hysteretic behaviour according to the extended Masing rule, as described by Kramer (1996).

An example of a hysteretic force-displacement curve is shown in Figure 6.

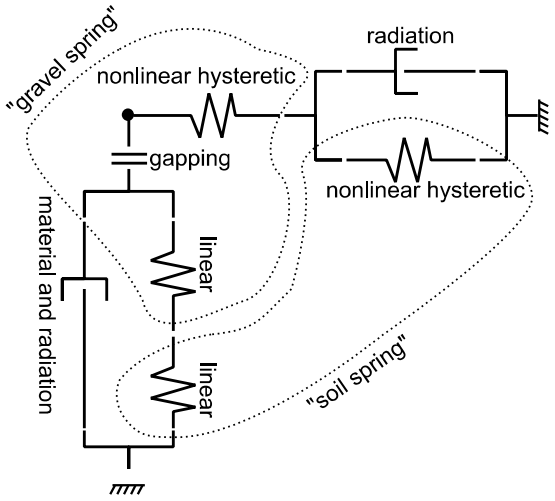

Figure 5. Detailed view of each set of distributed springs. The dotted loops show which elements are referred to as "gravel" and "soil" behaviour.

3.4 *Two-dimensional generalisation*

The terms "vertical" and "horizontal" are used in the above for springs and dashpots. While the vertical component involves no further complications, the horizontal springs and dashpots shall, however, be defined in the two horizontal dimensions. Since the springs are nonlinear and hysteretic, this definition is non-trivial.

The intended behaviour is obtained by actually applying in total eight non-linear springs, distributed in the horizontal plane. The concept is illustrated in Figure 7. The full angular space is covered by symmetry in the spring definitions.

4 DETERMINATION OF PARAMETERS

4.1 *Vertical gravel springs*

The linear vertical gravel springs are determined as

$$K_z = \frac{E_{\text{oed}} \cdot A_{\text{rep}}}{h_{\text{gravel}}} = \frac{105\ \text{MPa} \cdot A_{\text{rep}}}{3\ \text{m}} = 35\,\frac{\text{MN}}{\text{m}\cdot\text{m}^2} \cdot A_{\text{rep}}$$

where h_{gravel} and E_{oed} are the thickness and the oedometer modulus of the gravel bed. The oedometer modulus of 105 MPa corresponds to the unloading stiffness measured in plate loading tests of a comparable gravel bed.

4.2 *Vertical soil springs*

The linear vertical soil springs are calibrated such that the behaviour of the tower foundations under a vertical load plus an overturning moment in IBDAS matches that in a 2D plane strain finite element model in Plaxis. The Plaxis model considers both the gravel bed and the pile-reinforced subsoil and is shown in Figure 8.

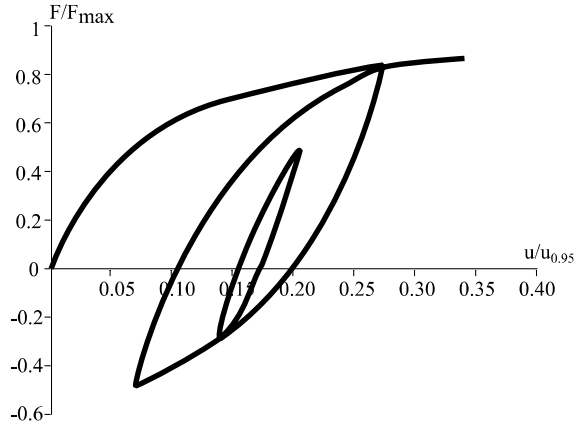

Figure 6. Hysteretic curve following Masing behaviour.

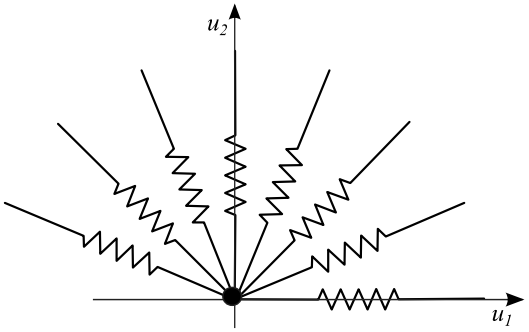

Figure 7. Discretized lateral F-u supports around each spring location, each representing a 1D non-linear F-u relation for their space angle.

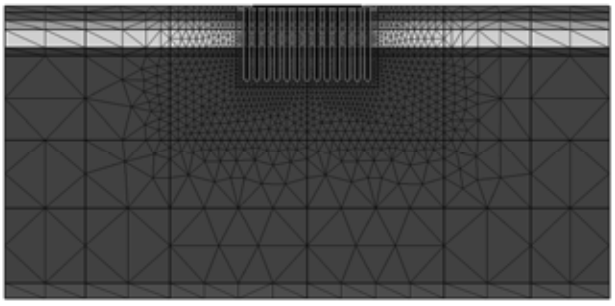

Figure 8. 2D Plaxis model, north tower.

Table 1. Material parameters, north tower.

ID	Top level [m]	γ [kN /m^3]	E [MPa]	φ [°]	s_u [kPa]	φ_{inter} [°]	c_{inter} [kPa]
Gravel	-40.0	18.0	78	45	-	51.5	-
N1	-43.0	17.5	411	40	-	28.0	-
N1A	-47.0	18.0	411	35	-	24.0	-
N2	-51.5	18.6	348	-	77 to 96	-	24.2 to 45.3
N3/5	-60.5	19.0	265	38	-	26.4	-
9	-64.5	18.9	239	-	104 to 341	-	53.6 to 214.3
10	-177.1 (to -184.7)	18.9	239	-	400		

Table 2. Material parameters, south tower.

ID	Top level [m]	γ [kN /m^3]	E [MPa]	φ [°]	s_u [kPa]	φ_{inter} [°]	c_{inter} [kPa]
Gravel	-40.0	18.0	77	45	-	51.5	-
S2	-43.0	17.6	203	-	41 to 70	-	10.7 to 41.4
S3	-59.5	18.9	78	33	-	22.3	-
S4	-63.5	18.9	161	-	107 to 137	-	54.3 to 80.8
5	-78.5	20.9	575	35	-		
6	-96.0	20.1	133	-	241 to 268		
7	-112.5	21.1	104	40	-		
8	-137.5 (to -200.0)	20.9	387	-	300		

All soils and the gravel bed are modelled with the Mohr-Coulomb material model with a Poisson's ratio $\nu = 0.3$. All soils are modelled as undrained materials using the effective strength parameter φ for sand layers and the undrained shear strength s_u for clay layers.

The gravel bed is modelled as a drained material. Stiffness values corresponding to the equivalent shear moduli from the site response analyses in ProShake are applied. Table 1 and 2 show the stiffness values for the NCE seismic event. For the FEE and SEE, the values are higher due to the lower strain levels in these seismic events.

The piles are modelled as linear elastic-perfectly plastic with equivalent stiffness parameters due to the 2D plane strain modelling. Plastic bending moments of 14.5 MNm and 22.2 MNm are defined in the models for the north and south tower, respectively, corresponding to the moments for which the characteristic structural capacities of the piles are fully utilized.

The base resistance of the 2 m diameter piles is assumed to be negligible. Shaft resistance is modelled using the interface strength parameters listed in Table 1 and 2. Undrained shear strength and consequently interface strength are defined as increasing from a value at the top of the layer to a value at the bottom of the layer. The interface strength parameters account for the differences between the actual geometry and the 2D plane strain approximation.

A reasonable agreement between the overturning behaviour in the IBDAS model and the 2D Plaxis model can be achieved with vertical soil spring stiffnesses of $K_z = 9.0\text{MPa/m} \cdot \text{A}_{\text{rep}}$ and $K_z = 4.5\text{MPa/m} \cdot \text{A}_{\text{rep}}$ at the north and south tower, respectively. This is illustrated for the north tower in Figure 9.

4.3 *Horizontal gravel springs*

A 3D finite element model in Abaqus is used to determine the load-displacement behaviour of the gravel bed. Exploiting symmetry, a 5 m wide, 2.5 m deep and 3 m high gravel body with one half of a pile is used to represent one pile in an infinitely large pile group, as shown in Figure 10.

The front, back and bottom face of the gravel body are constrained in normal direction, while repetitive boundary conditions (Law and Lam 2001) are applied to the left and right sides. The pile is only allowed to rotate around its base. Coulomb friction contact is modelled between the stiff caisson bottom slab and the gravel with a friction coefficient $\mu = 0.7$. Coulomb friction contact is also modelled between the inside and outside of the pile and the gravel with a friction coefficient $\mu = 0.4$.

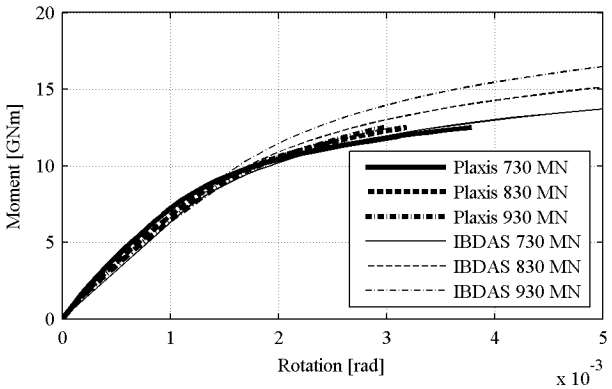

Figure 9. Calibration of vertical soil springs at the north tower by matching the overturning behaviour in the IBDAS model with the overturning behaviour in the 2D Plaxis model.

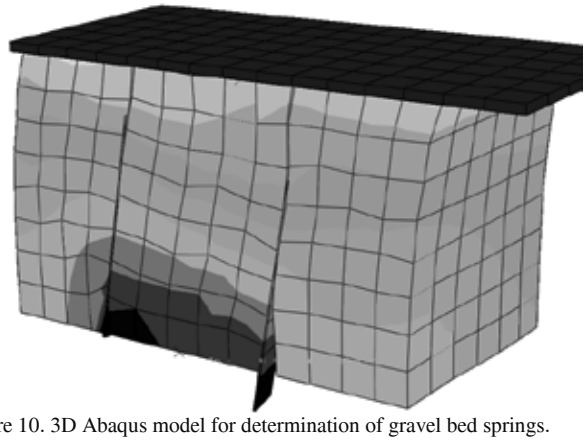

Figure 10. 3D Abaqus model for determination of gravel bed springs.

The Mohr-Coulomb material model with $\gamma' = 8$ kN/m^3, $E = 78$ MPa, $\nu = 0.3$, $\varphi = 45°$ and $\psi = 15°$ is used for the gravel. The pile is modelled as a rigid body. The load-displacement behaviour is determined by applying different vertical loads to the caisson bottom slab and pushing it in horizontal direction.

The hyperbolic backbone curves with $k_{h0,gravel} = 30$ MPa/m match the results from the 3D finite element model reasonably well, as shown in Figure 11.

4.4 *Horizontal soil springs*

The hyperbolic backbone curves of the horizontal soil springs are calibrated based on a vertical tower foundation load plus a horizontal force with a lever arm. The lever arm is chosen such that it represents the average observed lever arm in the seismic time history analyses with the global model.

A reasonable agreement between the push-over behaviour in the IBDAS model and the 2D Plaxis model can be achieved with an initial stiffness $k_{h0,soil} = 2.1\text{MPa/m}$ and a maximum shear stress $\tau_{max} = 0.70$ MPa at the north tower, cf. Figure 12, and $k_{h0,soil} = 0.35\text{MPa/m}$ and a maximum shear stress $\tau_{max} = 0.22$ MPa at the south tower.

4.5 *Dashpots*

The vertical distributed material and radiation dashpots have been derived based on linear elastic formulas given in Gazetas 1991 and the spring stiffness according to Section 4.2. The dashpot coefficients are $c_z = 0.97\text{MPa} \cdot \text{s/m} \cdot \text{A}_{\text{rep}}$ at the north tower and $c_z = 0.74\text{MPa} \cdot \text{s/m} \cdot \text{A}_{\text{rep}}$ at the south tower.

Similarly, based on Gazetas 1991 and the spring stiffness according to Section 4.4, the horizontal distributed radiation dashpot coefficients are determined as $c_y = 0.24\text{MPa} \cdot \text{s/m} \cdot \text{A}_{\text{rep}}$ at the north tower and $c_y = 0.11\text{MPa} \cdot \text{s/m} \cdot \text{A}_{\text{rep}}$ at the south tower.

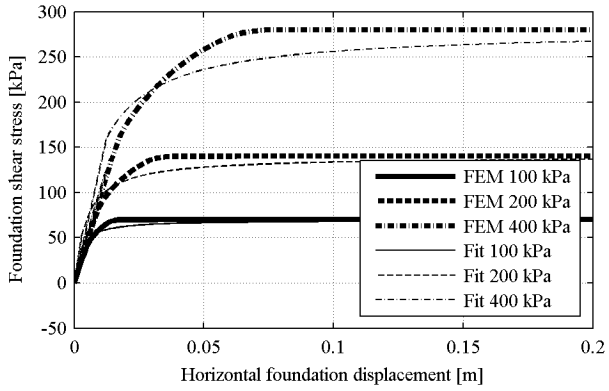

Figure 11. Load-displacement curves from the FE model and fitted hyperbolic backbone curves.

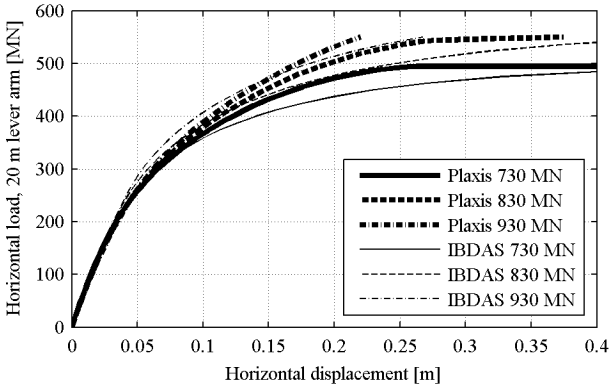

Figure 12. Calibration of horizontal soil springs at the north tower by matching the push-over behaviour in the IBDAS model with the push-over behaviour in the 2D Plaxis model.

5 RESULTS

5.1 *Relative displacements*

The relative displacement between the centre of the caisson and the free-field displacements of the soil is exemplified in Figure 13. Irreversible displacements of the caissons are clearly visible.

5.2 *Hysteretic behaviour*

The intended hysteretic behaviour is indeed produced in the finite element model, as it can be observed in Figure 14.

5.3 *Response in individual springs*

While the above curves illustrate the overall behaviour of the foundations, the response in individual soil and gravel springs can provide information on the *local* magnitude of displacement in

- the interface between soil and structure (gravel springs)
- the soil volume below the gravel bed (soil springs)

This distribution can be of importance for evaluating how onerous a plastic deformation is. The gravel spring can be considered ductile, where plastic deformation typically can be attributed to sliding in the gravel-foundation interface. In contrast, plastic deformation in the soil springs must typically be attributed to incipient yielding in the improved ground, and its magnitude should therefore be given great consideration.

An example of these displacements is shown in Figures 15 and 16. The spring is located at a foundation corner point, and the gapping behaviour in the gravel spring can be seen as stress-free displacements (horizontal parts of the dashed line at $\tau = 0$ in Figure 16). Further, it can be observed that at this location, the majority of the displacements occur in the gravel spring.

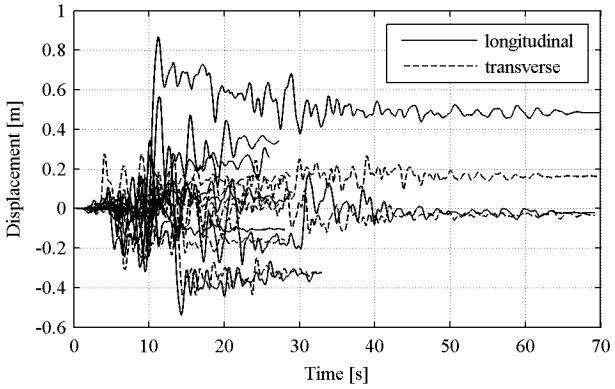

Figure 13. Relative displacement for seven NCE time histories, north tower.

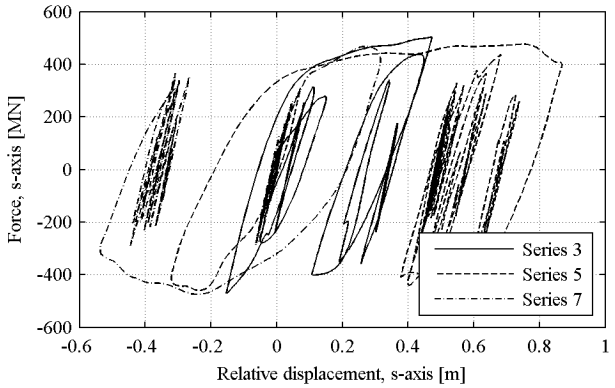

Figure 14. Force vs. relative displacement between foundation and soil in the bridge longitudinal direction. NCE seismic time histories, north tower.

The difference in the maximum value of the shear stress in the soil and gravel springs is due to the radiation dashpot in parallel with the horizontal soil spring, cf. Figure 5.

5.4 *Impact of non-linear effects*

To assess the consequences of allowing the soil-structure interface to undergo some plastic deformation, a comparative calculation with the global model is made, with the following changes:

- gapping elements deactivated
- all non-linear springs linearised with the initial stiffness
- horizontal material damping incorporated by dashpot

Thus, the soil-structure interface will behave fully linearly. The impact of this for the bridge structure can be assessed by observing the extreme moment envelope, which is plotted for the north tower in Figure 17.

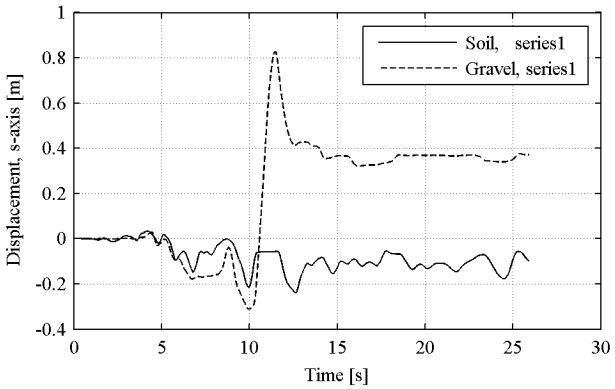

Figure 15. Bridge longitudinal displacements, NCE series 1, s-y- corner point, north tower.

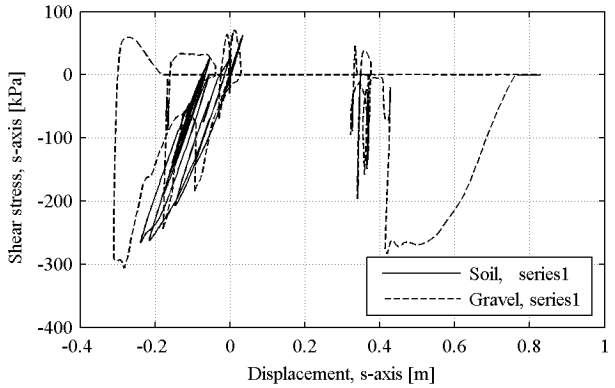

Figure 16. S-axial stress-displacement curves, NCE series 1, s-y- corner point, north tower.

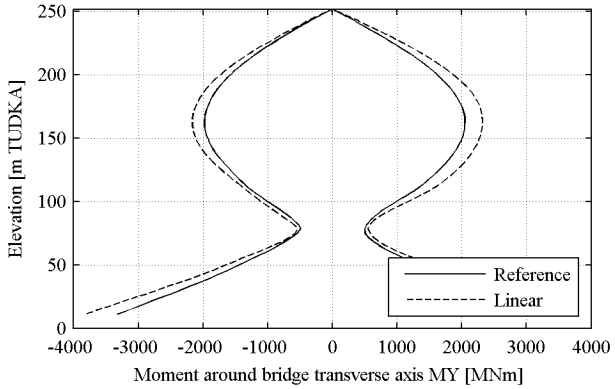

Figure 17. Envelopes of extreme moment in the north tower, NCE event, average of the seven series.

It should be noted that all design effects were evaluated as the average for the seven time histories, cf. EN 1998-1, clause 4.3.3.4.3(3). It can be observed that the linear soil interface in general provides more onerous moments in the north tower, on average 13% more than the reference interface which allows for some plastic deformation.

6 CONCLUSIONS

An advanced, non-linear model of the soil-structure interaction for the tower foundations has been established. The model includes distributed springs for three-dimensional dynamic analyses. Compared to single-point linear supports, this has the following benefits:

- Possibility to calculate distributed stresses under the foundation directly during time-history analyses
- Direct modelling of the horizontal shear capacity in the soil-structure interface, dependent on the interface friction coefficient and on the time-varying vertical force, $F_{H,res} < \mu \cdot F_z$.
- Thus, proper modelling of foundation gapping is also achieved, and the overall moment-rotation curve is directly made dependent on the vertical force.
- The shear stresses in the interface does also incorporate shear from torsional moment (M_z).
- Separate indication of displacements in the gravel bed/foundation interface and in the subsoil.
- Possibility to calibrate with pseudo-static continuum finite element models with good accuracy; also for varying vertical force, which normally is difficult.

Thus, by the detailed modelling of dynamic behaviour, it is possible to implement in a practical manner a displacement-based verification for large earthquakes, where seismic energy is dissipated by foundation rocking with gapping, some controlled and limited sliding and permanent horizontal displacements within the subsoil.

7 ACKNOWLEDGEMENTS

The authors gratefully acknowledge the permission by Owner NÖMAYG / Nurol-Özaltin-Makyol-Astaldi-Yüksel-Göçay and Contractor IHI Infrastructure Systems CO., Ltd. to publish this paper.

8 REFERENCES

Fédération internationale du béton (FIB) 2001. *Seismic bridge design and retrofit - structural solutions. State-of-art report.* Bulletin 39. Sprint-Digital-Druck, Stuttgart.

Gazetas G. 1991. Foundation vibrations, Chapter 15 in H. Y. Fang (Ed.): *Foundation Engineering Handbook.* Van Nostrand Reinhold, New York.

Kramer S. L. 1996. *Geotechnical earthquake engineering*. Prentice-Hall, New Jersey.

Law H.K. & Lam I.P. 2001. Application of periodic boundary for large pile group. *Journal of Geotechnical and Geoenvironmental Engineering* 127 (10), 889-892.

Lam I.P., Law H.K. and Martin G.R. 2007. *Bridge Foundations: Modeling Large Pile Groups and Caissons for Seismic Design*. Technical Report MCEER-07-0018, 12/1/2007. U. S. Department of transportation, Federal Highway Administration.

Sørensen K.A., Jakobsen P.F. and Andersen G.B. 1990. IBDAS, an integrated bridge design and analysis system. *3rd Int. Conf. on Short and Medium Span Bridges*, 105-116, Toronto.

Yang D., Dobry R. and Peck, R.B. 2001. Foundation-soil-inclusion interaction modeling for Rion-Antirion Bridge seismic analysis. *4th Int. Conf. on Recent Advances in Geotechnical Earthquake Engineering and Soil Dynamics*, San Diego.